

Evolution of Helimagnetic Correlations when approaching the Quantum Critical Point of $\text{Mn}_{1-x}\text{Fe}_x\text{Si}$

C. Pappas,¹ A. O. Leonov,² L.J. Bannenberg,¹ P. Fouquet,³ T. Wolf,⁴ and F. Weber^{4,5}

¹*Faculty of Applied Sciences, Delft University of Technology, Mekelweg 15, 2629 JB Delft, The Netherlands*

²*Chiral Research Center, Hiroshima University, Higashi Hiroshima, Hiroshima 739-8526, Japan**

³*Institut Laue Langevin, 71 Avenue des Martyrs, CS 20156, Grenoble, France*

⁴*Institute for Solid State Physics, Karlsruhe Institute of Technology, 76131 Karlsruhe, Germany*

⁵*Institute for Quantum Materials and Technologies,
Karlsruhe Institute of Technology, 76131 Karlsruhe, Germany*

(Dated: November 4, 2021)

We present a comprehensive investigation of the evolution of helimagnetic correlations in $\text{Mn}_{1-x}\text{Fe}_x\text{Si}$ with increasing doping. By combining polarised neutron scattering and high resolution Neutron Spin Echo spectroscopy we investigate three samples with $x=0.09, 0.11$ and 0.14 , i.e. with compositions on both sides of the concentration $x^* \sim 0.11$ where the helimagnetic Bragg peaks disappear and between x^* and the quantum critical concentration $x_C \sim 0.17$, where T_C vanishes. We find that the abrupt disappearance of the long range helical periodicity at x^* , does not affect the precursor fluctuating correlations. These build up with decreasing temperature in a similar way as for the parent compound MnSi. Also the dynamics bears strong similarities to MnSi. The analysis of our results indicates that frustration, possibly due to achiral RKKY interactions, increases with increasing Fe doping. We argue that this effect explains both the expansion of the precursor phase with increasing x and the abrupt disappearance of long range helimagnetic periodicity at x^* .

INTRODUCTION

The physics of the chiral magnet MnSi touches onto several fundamental questions in condensed-matter physics, from the stabilisation of exotic states like chiral skyrmions [1] to the interplay between localised and itinerant magnetism [2–8] as well as to non-Fermi liquid behaviour [9–14] and quantum fluctuations [15–23]. Under pressure a non-Fermi liquid behaviour sets-in without quantum criticality [11, 15, 24, 25]. Furthermore, the first order transition temperature T_C is driven to 0 K at $p_C \sim 1.4$ GPa, although the magnetic moment does not vanish. In the region of the temperature-pressure phase diagram, where $p \gtrsim p_C$ and $T_C = 0$ K, long range spiral and skyrmion correlations are restored under magnetic fields [7], a result that has been attributed to a softening of the magnetic moment. Pressure would therefore enhance the itinerant electron character of magnetism triggering the suppression of T_C . On the other hand, in the absence of quantum critical point (QCP) at p_C [19], the origin and nature of the highly debated non-Fermi liquid phase [16–18, 20, 26, 27] remains an open question. It was suggested that this phase, out of which magnetic fields induce long range spiral correlations is fluctuating and possibly of quantum nature [19]. However, our high resolution Neutron Spin Echo (NSE) spectroscopy measurements did not reveal the existence of such fluctuations, possibly due to limitations (background contribution of the pressure cell) inherent to measurements under high pressures [7].

These limitations are overcome by chemical pressure, in the form of Fe doping in $\text{Mn}_{1-x}\text{Fe}_x\text{Si}$. The behaviour of this system resembles that of MnSi under pressure [28–

37] and our magnetization, susceptibility and SANS investigations [28, 29] led to the phase diagram shown in Fig. 1. With increasing doping, the transition temperature decreases continuously and vanishes at $x_C \sim 0.17$. On the other hand, the helimagnetic Bragg peaks, a signature of long range helimagnetic periodicity, disappear abruptly at a much lower concentration of $x^* \sim 0.11$. For $x \gtrsim x^*$ magnetic susceptibility and electric transport phenomena reveal a non-Fermi liquid behaviour, which, as in MnSi under pressure, has been attributed to a chiral spin liquid state governed by quantum fluctuations [35–37]. Here we investigate the evolution of helimagnetic correlations and their dynamics as a function of chemical substitution in $\text{Mn}_{1-x}\text{Fe}_x\text{Si}$ using polarised neutron scattering and Neutron Spin Echo (NSE) spectroscopy. We investigated three samples with $x=0.09, 0.11$ and 0.14 , i.e. with compositions on both sides of x^* and between x^* and x_C . Our results reveal that the abrupt disappearance of long range helimagnetic periodicity at x^* does not affect the precursor fluctuating correlations. These build up with decreasing temperature in a way that is very similar to that of the parent compound MnSi. Also the dynamics, i.e. the characteristic relaxation times and their temperature dependence, resembles the behaviour of MnSi.

In order to understand these results we discuss the evolution of magnetic interactions with doping and also compare $\text{Mn}_{1-x}\text{Fe}_x\text{Si}$ with MnSi under pressure. Our analysis brings us to the conclusion that in $\text{Mn}_{1-x}\text{Fe}_x\text{Si}$ doping introduces frustration. We argue that this effect explains both the destabilisation of long range helimagnetic periodicity at x^* as well as the robustness of the precursor phase and its expansion with increasing x .

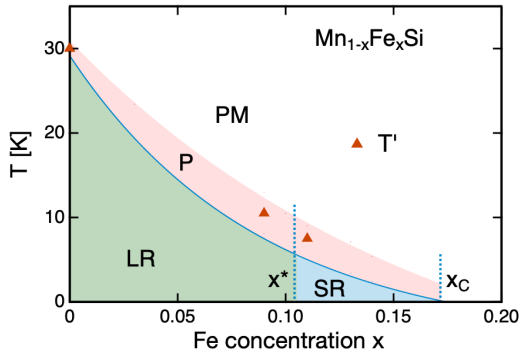


FIG. 1. Phase diagram of $\text{Mn}_{1-x}\text{Fe}_x\text{Si}$ deduced from our previous SANS and susceptibility measurements [28, 29]. The pink shaded area indicates the precursor phase, P, and PM stands for the paramagnetic phase. The blue line indicates the transition to the ordered helimagnetic phase with long (LR) and short (SR) range periodicity respectively. The temperatures T' have been determined as shown in Fig. 2 (b) and (c).

EXPERIMENTAL RESULTS

The samples were grown using the Bridgeman method. For $x=0.09$, 0.11 we measured the same single crystals as in our previous SANS study [28]. For $x=0.14$ and in order to compensate for the neutron intensity losses at this high Fe doping we chose a large polycrystalline and racemate polycrystalline sample, from the same batch as the samples of our previous studies [28, 29]. On one hand, this choice is not problematic, since at this composition the magnetic Bragg peaks have disappeared and the magnetic correlations are no longer pinned to the lattice. On the other hand, as it will be explained below, the polarised neutron scattering from this sample cannot be used to determine the degree of chirality of the magnetic correlations.

The measurements were performed at the IN11 spectrometer, of the Institut Laue Langevin, using the paramagnetic NSE configuration and an incoming wavelength of 0.55 nm. For each sample we determined the polarised neutron scattering and the NSE spectra at the respective maxima of the magnetic scattering intensity. These occur at the scattering vector values $Q=0.58$, 0.68 and 0.88 nm^{-1} leading to helical pitches $\ell=10.8$, 9.2 and 7.1 nm, for $x=0.09$, 0.11 and 0.14 respectively, in good agreement with our previous SANS results [28].

By exploiting the polarisation analysis capabilities of the experimental set-up we obtained an accurate determination of the magnetic scattering and of the chiral fraction of the magnetic correlations [38–43]. The results, shown in Fig. 2(b) and (c), highlight the abrupt change of behaviour at x^* .

For $x = 0.09$, i.e. for $x < x^*$, a jump of intensity marks the onset of the helimagnetic Bragg peaks and the

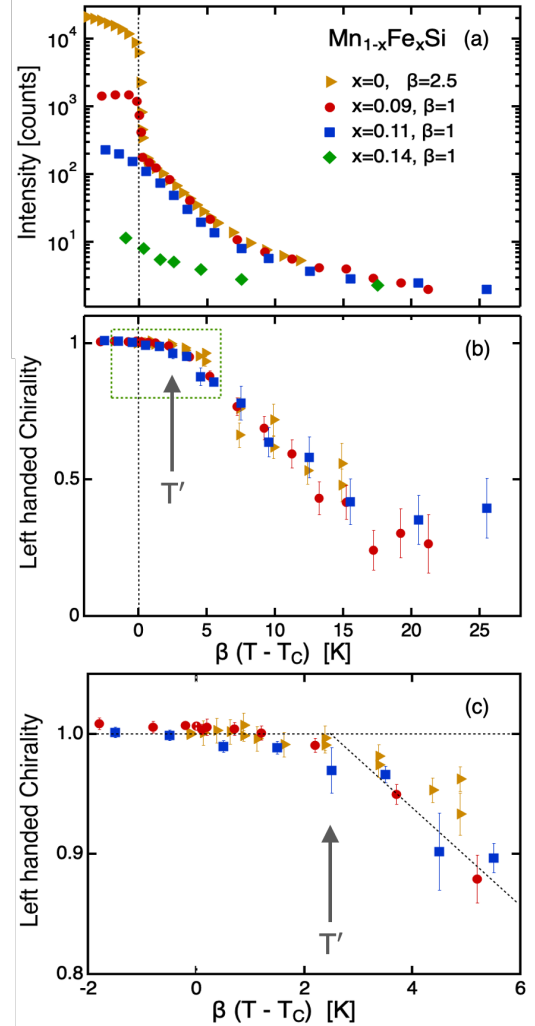


FIG. 2. Temperature dependence of the helimagnetic SANS intensity (a) and the left handed chiral fraction of the scattering (b) and (c). For the sake of comparison between the results of the three compositions investigated here and the parent compound MnSi, the abscissa is the scaled temperature difference $\beta(T - T_C)$, with $\beta=2.5$ for MnSi and $\beta = 1$ otherwise. In this way it is possible to account for the broadening of the precursor phase found for the doped samples. $T_C=7.8$, 5 and 2.5 K for $x=0.09$, 0.11 and 0.14 respectively. Panel (c) shows a close-up view of the green rectangle area shown in (b). The dotted lines in (c) illustrate the determination of at $T' \sim \beta(T - T_C)=2.5$. For $T < T'$ the scattering of MnSi, $\text{Mn}_{0.91}\text{Fe}_{0.09}\text{Si}$ and $\text{Mn}_{0.89}\text{Fe}_{0.11}\text{Si}$ reaches full left handed chirality within at least two times the error bars.

first order phase transition at $T_C = 7.8$ K. This jump disappears for $x > x^*$. However, for $x=0.11$ the precursor correlations build up with decreasing temperature in the same way as for $x=0.09$. Consequently, the precursor phase builds up in a similar way on both sides of x^* , a result that is hard to reconcile with the Brazovskii scenario proposed to explain the first order phase transition in MnSi and other chiral magnets [44]. For $x=0.14$, the

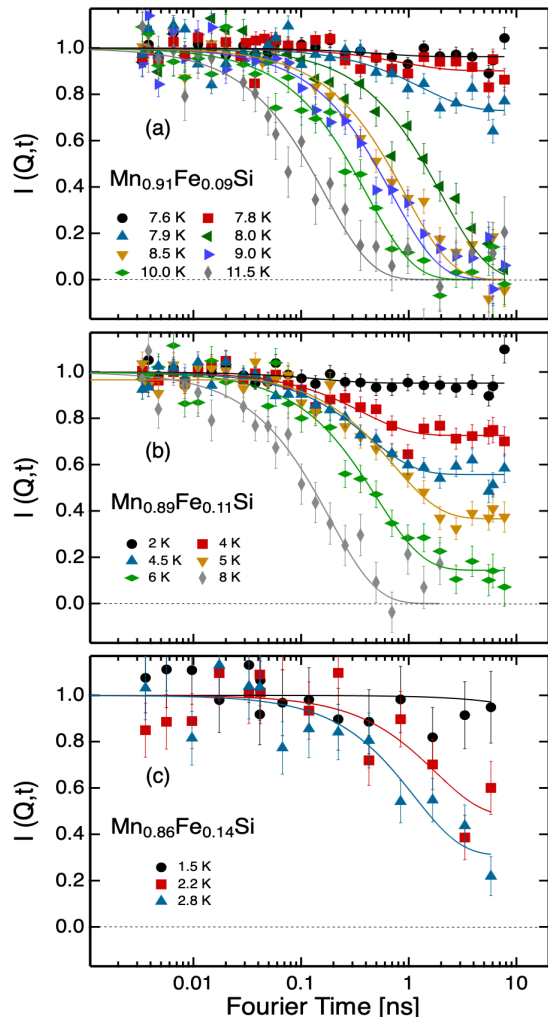


FIG. 3. Intermediate scattering functions, determined by Neutron Spin Echo spectroscopy, of $\text{Mn}_{0.91}\text{Fe}_{0.09}\text{Si}$ (a), $\text{Mn}_{0.89}\text{Fe}_{0.11}\text{Si}$ (b) and $\text{Mn}_{0.86}\text{Fe}_{0.14}\text{Si}$ (c). The lines represent fits to an exponential decay (see text).

evolution of intensity with temperature is much slower and can only be superimposed with data from lower dopings assuming a negative T_C .

Fig. 2 (b) and (c) shows that the scattering from both single crystalline samples, with $x = 0.09$ and 0.11 , is fully chiral at low temperatures. Unpublished results on single crystals indicate that the correlations remain chiral for dopings even higher than x_C [45]. However, the scattering from our 14% polycrystalline sample was achiral. This brought us to the conclusion that it is a racemate combining grains with different structural chirality, because in this system structural and magnetic chiralities are coupled [46]. Thus, the polarised neutron scattering from this sample does not reflect the chirality of magnetic correlations and for this reason this concentration is not included in Fig. 2 (b) and (c).

For $x = 0.09$ and 0.11 , full chirality extends up to

$T' \sim T_C + 2.5$ K, thus well above T_C . The temperature interval $T' - T_C$ is ~ 2.5 times broader than in MnSi, where full chirality is found up to $T' \sim T_C + 1$ K [42, 43]. In order to account for this difference when comparing the behaviour of the pristine and doped samples, the abscissas in Fig. 2 are the scaled temperature differences $\beta(T - T_C)$, with $\beta=2.5$ for MnSi and $\beta = 1$ otherwise. In these plots $\text{Mn}_{0.91}\text{Fe}_{0.09}\text{Si}$ reproduces the behaviour of MnSi, for both the intensity and the chiral fraction.

Further insight in the effect of chemical doping on the magnetic behaviour is provided by the intermediate scattering functions $I(Q = \tau, t)$, determined by NSE spectroscopy and shown in Fig. 3. The spectra follow an exponential decay that can be fitted by the function $I(Q = \tau, t) = (1 - a_{el}) \exp(-t/t_0) + a_{el}$, where t_0 is the characteristic relaxation time and a_{el} the elastic fraction of the scattering. This behaviour contrasts with that of other disordered helimagnets, such as $\text{Fe}_{0.7}\text{Co}_{0.3}\text{Si}$ [47, 48] or Zn doped Cu_2OSeO_3 [49], where strong deviations from exponentiality have been reported.

The exponential relaxation rules out a spin-glass-like ground state, the footprint of which would have been a stretched exponential decay [50, 51]. Furthermore, the NSE spectra become completely elastic at the base temperature, a result, which excludes the spin liquid scenario suggested for $x > x^*$ [35–37]. The elastic fraction, depicted in Fig. 4 (a), reflects the evolution of the scattered intensity shown in Fig.2(b). The change at T_C is almost step-like, characteristic of the first order phase transition, for MnSi and $\text{Mn}_{0.91}\text{Fe}_{0.09}\text{Si}$. On the other hand, for $x > x^*$, a_{el} increases gradually with decreasing temperature as also found in the disordered helimagnet $\text{Fe}_{0.7}\text{Co}_{0.3}\text{Si}$ [47].

The characteristic relaxation times, t_0 , depicted in Fig. 4 (b)-(c), do not change with doping and are comparable to those of MnSi [42, 43]. Their values vary between 0.1 and 2 ns, leading to characteristic energies, $\hbar\omega$, between $6.58 \mu\text{eV}$ and $0.33 \mu\text{eV}$. These values are much lower than those reported by a previous study [32], which however suffered from a low Q and energy resolution. The energies found here correspond to temperatures between 80 and 4 mK. Consequently, these are classical fluctuations, with $\hbar\omega \ll kT$, not the quantum fluctuations discussed in the literature [35–37]. Thus, classical critical slowing down prevails the dynamics of helimagnetic correlations for $x > x^*$ masking the quantum criticality associated with the putative QCP at x_C .

DISCUSSION

Our results show that Fe doping affects the first order transition and the long range helical periodicity in a very different way than the precursor phase. While the former disappear abruptly at x^* , the latter expands and persists up to higher dopings. Also the characteristic relaxation

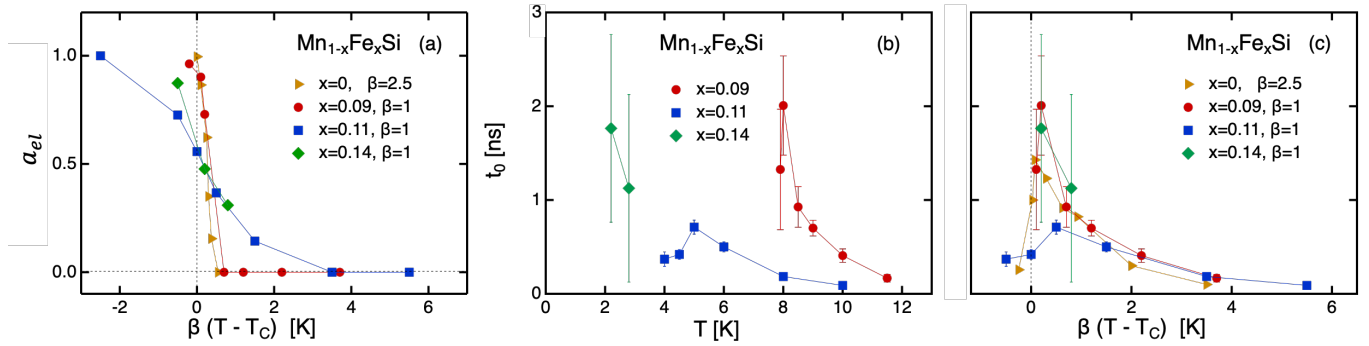


FIG. 4. Evolution with temperature and doping of the elastic fractions a_{el} and the characteristic times t_0 deduced from fitting an exponential decay to the NSE spectra of Fig. 3 (see text). In (a) and (c) the evolution of a_{el} and t_0 is compared with that of parent compound MnSi and for this reason the abscissa is, as in Fig. 2, the scaled temperature difference $\beta(T - T_C)$, with $\beta=2.5$ for MnSi and $\beta = 1$ otherwise.

times of the fluctuations are comparable to those found in MnSi. In order to understand these results and in particular the robustness of the precursor phase, we adopt the Dzyaloshinskii model for cubic non-centrosymmetric ferromagnets [52–54], which leads to the free energy per unit cell [55]:

$$\mathcal{E} = \frac{Ja^2}{2} \sum_{i=x,y,z} \partial_i \mathbf{m} \cdot \partial_i \mathbf{m} + Da \mathbf{m} \cdot \nabla \times \mathbf{m} - a^3 \mu_0 M \mathbf{m} \cdot \mathbf{H} + \mathcal{E}_a, \quad (1)$$

with J the ferromagnetic Heisenberg exchange, D the Dzyaloshinskii-Moriya (DMI) interaction, \mathbf{m} the unit vector in the direction of the magnetization, M the magnetization, a the lattice constant, and \mathcal{E}_a the magnetic anisotropy energy. The ground state consists of helical spirals with a periodicity of $\ell = 2\pi a J/D$ propagating along specific crystallographic directions fixed by magnetic anisotropy. A magnetic field strong enough to overcome the anisotropy, aligns the spirals towards its direction and tilts the magnetic moments by an angle given by $\cos \theta = H/H_{C2}$, where H_{C2} is the critical field above which the homogeneous or field-polarised state sets in. The model of Eq. 1 leads to $\mu_0 M_0 H_{C2} = D^2/Ja^3$, with M_0 the volume magnetization at H_{C2} . Therefore, at low temperatures, the pitch of the helical spirals can be written as: $\ell = 2\pi a \sqrt{J/(a^3 \mu_0 M_0 H_{C2})}$ and by assuming that J is given by the Curie-Weiss temperature, T_{CW} (mean field approximation), it can be derived from quantities that have been determined experimentally (see e.g. Table 1 of [29]). In particular the lattice constant, a , does not change significantly with temperature [11] but varies linearly with x , between 0.4565 nm for MnSi and 0.449 nm for FeSi [46].

By combining this experimental input we calculate the values of ℓ that are depicted in Fig. 5 and vary very little with doping. For the parent compound MnSi the relative difference between the experimental and calculated values of ℓ does not exceed 6%, which gives confidence

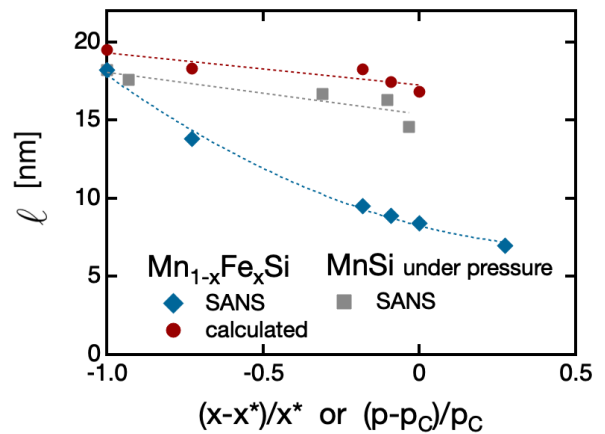


FIG. 5. Evolution of the helical pitch as a function of Fe doping, in the case of $\text{Mn}_{1-x}\text{Fe}_x\text{Si}$, or as a function of pressure, in the case of MnSi. For the sake of comparison the abscissa is either the relative doping $(x - x^*)/x^*$ for $\text{Mn}_{1-x}\text{Fe}_x\text{Si}$, or the relative pressure $(p - p_C)/p_C$ for MnSi. The red dots have been calculated for $\text{Mn}_{1-x}\text{Fe}_x\text{Si}$ using the model of Eq. 1.

to our approach. For the sake of comparison Fig. 5 also shows the pressure dependence of ℓ for MnSi (data from Fig. 2(e) of [7]), which is weak and follows the trend of the calculated values. This contrasts with the behaviour of $\text{Mn}_{1-x}\text{Fe}_x\text{Si}$, where ℓ decreases rapidly with increasing Fe doping. At $x=0.11$, the highest Fe concentration where it was still possible to determine both M_0 and H_{C2} , the experimental value of ℓ is half the one expected from the model of Eq. 1.

An even more drastic reduction of the helical periodicity was recently found in $\text{MnSi}_{1-x}\text{Ge}_x$ [56, 57] and has been attributed to frustration [58]. The effect of frustration can be explained by the interplay between the DMI and higher-order derivatives terms in Eq. 1. These were the original skyrmion stabilisation mechanism consid-

ered by Skyrme [59] and lead to an attracting skyrmion-skyrmion or soliton-soliton interaction [60]. The numerical simulations in [58] reveal a drastic decrease of ℓ in the presence of an additional antiferromagnetic exchange J_{AF} term in Eq. 1. This reduction occurs even for weak frustration and, although it was not possible to derive an analytical expression of general validity, the limit $\ell \gg a$, leads to [58]:

$$\ell \approx 2\pi a \frac{J}{D} \left(1 - 4 \frac{J_{AF}}{J} \right). \quad (2)$$

Following this approximation for $\text{Mn}_{0.89}\text{Fe}_{0.11}\text{Si}$, where $\ell/a \approx 18$, the 50% pitch reduction leads to $J_{AF}/J \approx 1/8$. This relatively low ratio points to weak frustration and is consistent with the weak disorder seen by electron spin resonance [61] and the exponential relaxation of the NSE spectra.

Antiferromagnetic interactions may result from oscillatory RKKY exchange between localised magnetic moments, as suggested by the analysis of the ordinary and anomalous Hall effects [62]. These achiral interactions increase with increasing x and this effect would explain the destabilisation of the helical periodicity at x^* . It was suggested that RKKY interactions arise from the modification of the electron and hole concentrations by the substitution of Mn by Fe [62]. Thus, similarly to MnSi under pressure, the modification of the electronic state drives the destabilisation of the long range helical order and of the sharp first order phase transition at T_C . However, the specific microscopic mechanisms are different for the two systems as highlighted by the evolution of the helical pitch ℓ shown in Fig. 5. Frustration and disorder are important for $\text{Mn}_{1-x}\text{Fe}_x\text{Si}$ in contrast to MnSi under pressure.

Frustration can stabilise spiral and skyrmion periodic states [60, 63] but, unlike DMI, it does not impose the chirality i.e. it does not impose a sense of rotation. This leads to rich phase diagrams, with phases that are impossible in chiral magnets. The competition between frustration and DMI, however, has only been touched upon in the literature [58, 64, 65] and only in the low-temperature regime with a fixed magnetization modulus. In fact, the influence of frustration on the phase transition and the precursor states in chiral magnets is a most challenging and unresolved problem, which we approach based on general considerations.

Near the ordering temperatures, the functional of Eq. 1 must be supplemented by the Landau expansion in powers of the magnetization [54]:

$$W_0 = A(T - T_0)M^2 + BM^4, \quad (3)$$

where $B > 0$ and T_0 is the ferromagnetic ordering temperature, i.e. the Curie temperature in the absence of DMI. Under the influence of temperature and of an applied magnetic field, this term enables variations of the magnetization amplitude, which lead to sizeable effects in the vicinity of T_C , the transition temperature in the presence of DMI. In the precursor region of chiral mag-

nets, the chiral twisting is accompanied by strong longitudinal modulations of the magnetization and its interplay with rotational modes [17, 66–68]. Thus, anomalous spin-textures can be expected such as a staggered half-skyrmion lattice [17] - a close analogue of the square lattice of merons in frustrated magnets [69]. Even in the absence of frustration these precursor modulated states may have both senses of magnetization rotation. However, the modulus increases or decreases depending on whether the rotation adopts the correct or the wrong rotational sense [67, 70] with the correct chirality eventually dominating close to T_C , as shown in Fig.2. This mechanism induces fan-like oscillations of isolated skyrmions [67] and solitons [70] and leads to their attracting interaction with potentials containing a plethora of local minima at different mutual distances.

An increasing frustration will amplify these precursor modulations and will thus enhance and expand the precursor region, as it is indeed the case for $\text{Mn}_x\text{Fe}_{1-x}\text{Si}$ [28–32].

CONCLUSION

To conclude, our results shed light on the evolution of helimagnetic correlations and fluctuations in $\text{Mn}_{1-x}\text{Fe}_x\text{Si}$ for $x < x_C$. On one hand, our observations rule out both the spin liquid and the quantum fluctuations hypothesis for $x > x^*$, which cannot be associated with a quantum critical point. On the other hand, our analysis indicates that, with increasing doping, frustration increases, which we attribute to increasing competition between chiral DMI and achiral RKKY interactions. We argue that frustration explains the expansion of the precursor phase for $x < x_C$ and the destabilisation of the long range helimagnetic periodicity at x^* .

More generally, both frustration and DMI can stabilise spiral and skyrmion periodic states, and the competition between the two can lead to rich phase diagrams with new phases and spin configurations, providing a fertile ground for future developments.

ACKNOWLEDGMENTS

C.P. thanks S.V. Grigoriev for useful discussions and for sharing unpublished experimental results. The experiments were performed at the Institut Laue Langevin, France, and the data are available at <https://doi.ill.fr/10.5291/ILL-DATA.4-03-1729>. The single crystals were aligned at the OrientExpress instrument with the support of Bachir Ouladdiaf. The work of L.J.B. and C.P. has been financially supported by The Netherlands Organization for Scientific Research through Project No. 72 1.012 .102 (Larmor). CP acknowledges

travel support from JSPS KAKENHI Grant Number JP15H05882 (J-Physics).)

* c.pappas@tudelft.nl

- [1] S. Mühlbauer, B. Binz, F. Jonietz, C. Pfleiderer, A. Rosch, A. Neubauer, R. Georgii, and P. Böni, *Science* **323**, 915 (2009).
- [2] Y. Ishikawa, G. Shirane, J. A. Tarvin, and M. Kohgi, *Phys. Rev. B* **16**, 4956 (1977).
- [3] C. Thessieu, J. Flouquet, G. Lapertot, A. N. Stepanov, and D. Jaccard, *Solid State Communications* **95**, 707 (1995).
- [4] M. Corti, F. Carbone, M. Filibian, T. Jarlborg, A. A. Nugroho, and P. Carretta, *Phys. Rev B* **75**, 115111 (2007).
- [5] S. V. Demishev, A. V. Semeno, A. V. Bogach, V. V. Glushkov, N. E. Sluchanko, N. A. Samarin, and A. L. Chernobrovkin, *JETP Letters* **93**, 213 (2011).
- [6] H. Yasuoka, K. Motoya, M. Majumder, S. W. J. o. t. Physical, and 2016, *journals.jps.jp* **85**, 073701 (2016).
- [7] L. J. Bannenberg, R. Sadykov, R. M. Dalgliesh, C. Goodway, D. L. Schlagel, T. A. Lograsso, P. Falus, E. Lelièvre-Berna, A. O. Leonov, and C. Pappas, *Phys. Rev B* **100**, 054447 (2019).
- [8] A. Yaouanc, P. Dalmas de Réotier, B. Roessli, A. Maisuradze, A. Amato, D. Andreica, and G. Laperot, *Phys. Rev. Research* **2**, 013029 (2020).
- [9] C. Pfleiderer, S. Julian, and G. G. Lonzarich, *Nature* **414**, 427 (2001).
- [10] N. Doiron-Leyraud, I. R. Walker, L. Taillefer, M. J. Steiner, S. R. Julian, and G. G. Lonzarich, *Nature* **425**, 595 (2003).
- [11] C. Pfleiderer, P. Böni, T. Keller, U. K. Rößler, and A. Rosch, *Science* **316**, 1871 (2007).
- [12] M. Lee, W. Kang, Y. Onose, Y. Tokura, and N. P. Ong, *Phys. Rev. Lett.* **102**, 186601 (2009).
- [13] R. Ritz, M. Halder, M. Wagner, C. Franz, A. Bauer, and C. Pfleiderer, *Nature* **497**, 231 (2013).
- [14] T. R. Kirkpatrick and D. Belitz, *Phys. Rev B* **97**, 064411 (2018).
- [15] C. Pfleiderer, G. J. McMullan, S. R. Julian, and G. G. Lonzarich, *Phys. Rev. B* **55**, 8330 (1997).
- [16] S. Tewari, D. Belitz, and T. R. Kirkpatrick, *Phys. Rev. Lett.* **96**, 047207 (2006).
- [17] U. K. Rößler, A. N. Bogdanov, and C. Pfleiderer, *Nature* **442**, 797 (2006).
- [18] J. M. Hopkinson and H.-Y. Kee, *Phys. Rev. B* **79**, 14421 (2009).
- [19] C. Pfleiderer, A. Neubauer, S. Mühlbauer, F. Jonietz, M. Janoschek, S. Legl, R. Ritz, W. Münzer, C. Franz, P. G. Niklowitz, T. Keller, R. Georgii, P. Böni, B. Binz, A. Rosch, U. K. Rößler, and A. N. Bogdanov, *Journal of Physics-Condensed Matter* **21**, 164215 (2009).
- [20] T. R. Kirkpatrick and D. Belitz, *Phys. Rev. Lett.* **104**, 256404 (2010).
- [21] K.-Y. Ho, T. R. Kirkpatrick, Y. Sang, and D. Belitz, *Phys. Rev. B* **82**, 134427 (2010).
- [22] F. Krüger, U. Karahasanovic, and A. G. Green, *Phys. Rev. Lett.* **108**, 067003 (2012).
- [23] A. A. Povzner, A. G. Volkov, and T. A. Nogovitsyna, *Physica B: Physics of Condensed Matter* **536**, 408 (2018).
- [24] C. Pfleiderer, D. Reznik, L. Pintschovius, H. v Lohneysen, *et al.*, *Nature* **427**, 227 (2004).
- [25] L. Pintschovius, D. Reznik, C. Pfleiderer, and H. von Löhneysen, *Pramana* **63**, 117 (2004).
- [26] B. Binz, A. Vishwanath, and V. Aji, *Phys. Rev. Lett.* **96**, 207202 (2006).
- [27] I. Fischer, N. Shah, and A. Rosch, *Phys. Rev B* **77**, 024415 (2008).
- [28] L. J. Bannenberg, R. M. Dalgliesh, T. Wolf, F. Weber, and C. Pappas, *Phys. Rev. B* **98**, 184431 (2018).
- [29] L. J. Bannenberg, F. Weber, A. J. E. Lefering, T. Wolf, and C. Pappas, *Phys. Rev. B* **98**, 184430 (2018).
- [30] A. Bauer, A. Neubauer, C. Franz, W. Münzer, M. Garst, and C. Pfleiderer, *Phys. Rev. B* **82**, 064404 (2010).
- [31] S. V. Grigoriev, V. A. Dyadkin, E. V. Moskvin, D. Lamago, T. Wolf, H. Eckerlebe, and S. V. Maleyev, *Phys. Rev. B* **79**, 144417 (2009).
- [32] S. V. Grigoriev, E. V. Moskvin, V. A. Dyadkin, D. Lamago, T. Wolf, H. Eckerlebe, and S. V. Maleyev, *Phys. Rev. B* **83**, 224411 (2011).
- [33] C. Franz, F. Freimuth, A. Bauer, R. Ritz, C. Schnarr, C. Duvinage, T. Adams, S. Blügel, A. Rosch, Y. Mokrousov, *et al.*, *Phys. Rev. Lett.* **112**, 186601 (2014).
- [34] A. E. Petrova, S. Y. Gavrilkina, D. Menzel, and S. M. Stishov, *Phys. Rev B* **100**, 094403 (2019).
- [35] S. V. Demishev, A. N. Samarin, V. V. Glushkov, M. I. Gilmanov, I. I. Lobanova, N. A. Samarin, A. V. Semeno, N. E. Sluchanko, N. M. Chubova, V. A. Dyadkin, and S. V. Grigoriev, *JETP Letters* **100**, 28 (2014).
- [36] S. V. Demishev, A. N. Samarin, J. Huang, V. V. Glushkov, I. I. Lobanova, N. E. Sluchanko, N. M. Chubova, V. A. Dyadkin, S. V. Grigoriev, M. Y. Kagan, *et al.*, *JETP letters* **104**, 116 (2016).
- [37] J. Kindervater, T. Adams, A. Bauer, F. X. Haslbeck, A. Chacon, S. Mühlbauer, F. Jonietz, A. Neubauer, U. Gasser, G. Nagy, N. Martin, W. Häußler, R. Georgii, M. Garst, and C. Pfleiderer, *Phys. Rev. B* **101**, 104406 (2020).
- [38] M. Blume, *Phys. Rev.* **130**, 1670 (1963).
- [39] S. V. Maleyev, V. G. Baryakhtar, and P. A. Suris, *Sov. Phys. Solid State* **4**, 2533 (1963).
- [40] A. P. Murani and F. Mezei, in *Neutron Spin Echo* (Lecture Notes in Physics, vol 128. Springer, Berlin, Heidelberg, 1980) p. 104.
- [41] C. Pappas, G. Ehlers, and F. Mezei, in *Neutron Scattering from Magnetic Materials*, edited by T. Chatterji (Elsevier, 2006) p. 521.
- [42] C. Pappas, E. Lelièvre-Berna, P. Falus, P. M. Bentley, E. Moskvin, S. Grigoriev, P. Fouquet, and B. Farago, *Phys. Rev. Lett.* **102**, 197202 (2009).
- [43] C. Pappas, E. Lelièvre-Berna, P. Bentley, P. Falus, P. Fouquet, and B. Farago, *Phys. Rev. B* **83**, 224405 (2011).
- [44] M. Janoschek, M. Garst, A. Bauer, P. Krautscheid, R. Georgii, P. Böni, and C. Pfleiderer, *Phys. Rev. B* **87**, 134407 (2013).
- [45] S. V. Grigoriev, private communication.
- [46] S. V. Grigoriev, D. Chernyshov, V. A. Dyadkin, V. Dmitriev, E. V. Moskvin, D. Lamago, T. Wolf, D. Menzel, J. Schoenes, S. V. Maleyev, and H. Eckerlebe, *Phys. Rev. B* **81**, 012408 (2010).
- [47] L. J. Bannenberg, K. Kakurai, P. Falus, E. Lelièvre-Berna, R. M. Dalgliesh, C. D. Dewhurst, F. Qian,

- Y. Onose, Y. Endoh, Y. Tokura, and C. Pappas, *Phys. Rev. B* **95**, 144433 (2017).
- [48] L. J. Bannenberg, A. J. E. Lefering, K. Kakurai, Y. Onose, Y. Endoh, Y. Tokura, and C. Pappas, *Phys. Rev. B* **94**, 134433 (2016).
- [49] M. T. Birch, R. Takagi, S. Seki, M. N. Wilson, F. Kagawa, A. Štefanič, G. Balakrishnan, R. Fan, P. Steadman, C. J. Ottley, M. Crisanti, R. Cubitt, T. Lancaster, Y. Tokura, and P. D. Hatton, *Phys. Rev. B* **100**, 014425 (2019).
- [50] R. M. Pickup, R. Cywinski, C. Pappas, B. Farago, and P. Fouquet, *Phys. Rev. Letters* **102**, 097202 (2009).
- [51] C. Pappas, F. Mezei, G. Ehlers, P. Manuel, and I. A. Campbell, *Phys. Rev. B* **68**, 054431 (2003).
- [52] I. E. Dzyaloshinskii, *Soviet Physics JETP* **19**, 960 (1964).
- [53] I. E. Dzyaloshinskii, *Soviet Physics JETP* **20**, 665 (1965).
- [54] P. Bak and M. H. Jensen, *Journal of Physics C: Solid State Physics* **13**, L881 (1980).
- [55] F. Qian, L. J. Bannenberg, H. Wilhelm, G. Chaboussant, L. M. DeBeer-Schmitt, M. P. Schmidt, A. Aqeel, T. T. M. Palstra, E. H. Brück, A. J. E. Lefering, C. Pappas, M. Mostovoy, and A. O. Leonov, *Science Advances* **4**, eaat7323 (2018).
- [56] T. Tanigaki, K. Shibata, N. Kanazawa, X. Yu, Y. Y. Onose, H. S. Park, D. Shindo, and Y. Tokura, *Nano Letters* **15**, 5438 (2015).
- [57] Y. Fujishiro, N. Kanazawa, T. Nakajima, X. Z. Yu, K. Ohishi, Y. Kawamura, K. Kakurai, T. Arima, H. Mitamura, A. Miyake, K. Akiba, M. Tokunaga, A. Matsuo, K. Kindo, T. Koretsune, R. Arita, and Y. Tokura, *Nature Communications* **10**, 1059 (2019).
- [58] T. T. J. Mutter, A. O. Leonov, and K. Inoue, *Phys. Rev. B* **100**, 060407(R) (2019).
- [59] T. H. R. Skyrme, *Proceedings of the Royal Society London A* **260**, 127 (1961).
- [60] A. O. Leonov and M. Mostovoy, *Nature Communications* **6**, 8275 (2015).
- [61] S. V. Demishev, I. I. Lobanova, V. V. Glushkov, T. V. Ischenko, N. E. Sluchanko, V. A. Dyadkin, N. M. Potapova, and S. V. Grigoriev, *JETP Letters* **98**, 829 (2013).
- [62] V. V. Glushkov, I. I. Lobanova, V. Y. Ivanov, V. V. Voronov, V. A. Dyadkin, N. M. Chubova, S. V. Grigoriev, and S. V. Demishev, *Phys. Rev. Lett.* **115**, 256601 (2015).
- [63] T. Kurumaji, T. Nakajima, M. Hirschberger, A. Kikkawa, Y. Yamasaki, H. Sagayama, H. Nakao, Y. Taguchi, T.-h. Arima, and Y. Tokura, *Science* **365**, 914 (2019).
- [64] S. von Malottki, B. Dupé, P. F. Bessarab, A. Delin, and S. Heinze, *Scientific reports* **9**, 12299 (2019).
- [65] H. Y. Yuan, O. Gomonay, and M. Kläui, *Phys. Rev B* **96**, 134415 (2017).
- [66] V. Laliena, J. Campo, and Y. Kousaka, *Phys. Rev B* **94**, 094439 (2016).
- [67] A. O. Leonov and A. N. Bogdanov, *New Journal of Physics* **20**, 043017 (2018).
- [68] M. Shinozaki, S. Hoshino, Y. Masaki, A. N. Bogdanov, A. O. Leonov, J.-I. Kishine, and Y. Kato, *arXiv.org*, arXiv:1705.07778 (2017), 1705.07778.
- [69] Y. A. Kharkov, O. P. Sushkov, and M. Mostovoy, *Phys. Rev. Lett.* **119**, 207201 (2017).
- [70] B. Schaub and D. Mukamel, *Phys. Rev B* **32**, 6385 (1985).